Exploring the use-case for low-cost solid state LiDAR in automotive safety

James O'Donohoe

October 2024

Abstract

When one thinks of LiDAR in an automotive context, they often think of cutting edge 360 degree, single photon LiDAR systems that cost more than most cars. Yet these are still held back by the software and computational power they require. A lower cost solid state system stands a better chance of making it to the mass market and improving road safety for all. I investigated the use of such a system, characterised it's performance, and investigated how it's data could be used more effectively to improve safety. I found its accuracy to be more than satisfactory for a potential use case, though some concerns arose when separating objects from their environment was required.

Contents

1 Introduction

There aim of this project is to explore how low-cost LiDAR can used to improve automotive safety. Though there are far more advanced LiDAR systems, the cost is prohibitive and the computing power needed to process their data live in order to make any decisions, is still at the cutting edge.

The Project will be broken down into three key focuses:

1. Investigating using off the shelf, solid state LiDAR units
2. Testing their performance
3. Exploring different ways of using their raw data to improve their effectiveness

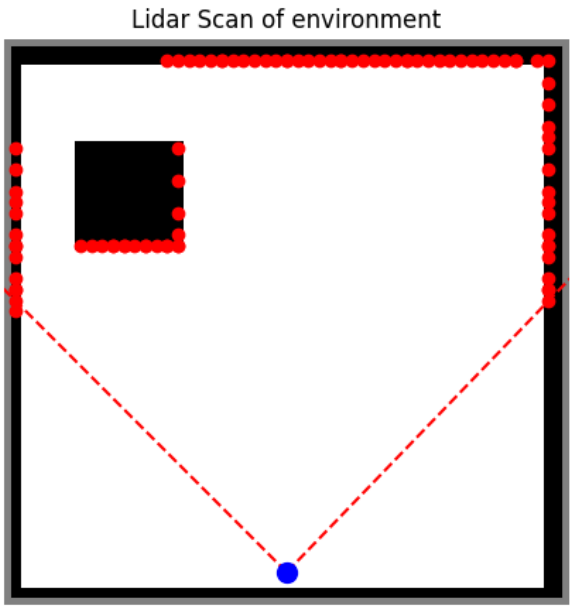

Figure 1: Idealised 2D Scenario

1.1 LiDAR in 2D

The most simple case of a LiDAR working in 2D, is to imagine a singular photon being emitted, and returning exactly along its incident path to a receiver at the same point as the emitter. The time of flight (ToF), would describe the distance of the first object along that path. By increasing the angle of incidence θ, by infinitesimal angle $\delta\theta$, a two dimensional view of the surroundings would be formed.

(Fig 1) shows the result of a such a system, where θ has been varied through 90 ° at 1° intervals. It is important to note the shadow (black box in upper left of fig 1) caused by the object in the LiDARs view, which make separating objects from their environment difficult.

Like all idealisations, there are some limitations when applied to reality. Though its possible to spin a LiDAR like this around to map the environment, it is both costly and and introduces vulnerable moving parts, which are sensitive to vibrations. For many practical applications such as on cars, a solid state system with no moving parts is preferred. The example of solid-state LiDAR used for these experiments works by emitting a diverging beam of light, which will usually be infrared, which triggers a digital timer. The light interacts with its surroundings, and then is reflected almost exactly along its path to a matrix of detectors

which can be a single line or a 2D array. In the case of 2D LiDAR this is a linear array of detectors. When the detector is activated it stops the timer started by the initial pulse of the laser, and returns a ToF.

1.2 Background context

Investigating the use of off the shelf LiDAR units.

1.2.1 Autonomous driving

The first thought when talking about LiDAR and cars is autonomous driving. However, this is as of yet unachieved, largely limited by computing and data rather than sensors. Better sensors can make things easier but not possible; in fact, the best in progress attempt at self-driving is Tesla based on a model of making it as widespread as possible, which relies on cheaper sensors rather than better ones. Although one could look at Wamo, the self-driving car company, who have taken a very different approach of using very expensive sensors to locate their position in the environment, and even better quality maps of the limited environment they can use, which they can then position themselves in. [1] This removes a lot of uncertainty and improves the capabilities of these self-driving cars. There are two main problems with this approach. One is the cost of the car, estimated at $250,000-$300,000 [2]. The second problem is the mapped environment. Everyone appreciates the effectiveness of google street-view, but it wasn't so long ago that a lot of places weren't mapped long into the projects existence, and anyone in a rural area knows how infrequently their maps are updated. Regardless, the focus of this is safety and affordability, so this approach does not align with that.[3] [4]

1.2.2 Comparing to 3D and 360 vision

3D LiDAR has its advantages for this focus, and its important to be aware of the tradeoffs we will be making by not using it. 3D when placed on top of a car can see over some objects in the road, depending on the height of its position, it could easily be possible to see over a pedestrian, and predict their depth and narrow down their exact location, making it easier to identify what they are. Compared to 2D LiDAR which can only determine if they are in a given angular sector, and has no height information. If you imagine trying to navigate the world with your vision being a 2D sum where each column of sight is summed into a total intensity , it would be very difficult to identify a person.

360 degree is another useful consideration. 360 degree spinning LiDARs allow for

infinitesimal angle readings. Assuming the beam is non-diverging and approximately infinitesimal receiver, by spinning it around and seeing what comes back, you can create a high definition map. There are issues with the vibrations and larger shocks of driving a vehicle with such a sensitive system, which can be accounted for at the expense of complexity and great cost.

The best way to eliminate these is a solid state LiDAR, these are (relatively) cheap, reliable, not prone to vibrations or acceleration, and can still be incredibly accurate. However they come at the cost of wide angular detectors, and limited data. For example the LiDAR used in these experiments has 16 segments of 3 degrees each, resulting in a total angular view of 48 degrees.

The challenge is to see if such a detector, or combination of two detectors, can locate a pedestrian accurately enough to be useable. To have confidence as to whether they are in the path of the vehicle or not, and to determine their locations accurately enough that when compared with a future sample, it can determine the direction of travel, and the errors of these readings won't allow the possibility of the pedestrian to have gone one way when they've in fact gone the other.

2 Theory

This Theory section covers some basic theory about light and its relevent phenomena with respect to LiDAR, as well as further theory about LiDAR itself, and Leddartech who manufacture the subject of the experiments in this thesis.

2.1 Light

Infrared light exists on the EM spectrum between 780nm at the edge of the visible spectrum and 1mm adjacent to the microwave region.[5] At 905nm, Leddarteks LEDDAR M16-LSR laser fits in the near infra-red region. There are many benefits and drawbacks to using this wavelength. It allows for the use of silicon-based sensors, which have a high sensitivity at a low cost.[6] However being close to the visible spectrum, and other ambient light sources such as the sun, brings about an abundance of opportunity for noise and interference. 1,550nm wavelength is becoming popular in LiDAR for this reason, as well as having a lower risk of eye damage for the same power. Within the same safety restrictions higher powers or more concentrated beams can be used allowing for longer ranging distances and clearer signals [7].

2.2 Reflection

LiDAR ranging is based on the reflection of light from the incident object. There are two categories of reflection; diffuse and specular. Specular refers to the familiar case where the angle of incidence is equal to the angle of reflection, and all reflected light is preserved along that path. Diffuse reflection on the other hand refers to the scattering of light in all directions from the point of incidence, resulting in a much greater loss in intensity. [8]

Specular often occurs at the surface of a transparent or reflective surface such as glass, water, or metal, and is therefore highly relevant when considering other cars on the road, but less so for pedestrians. It allows for cars to be observed at greater distances when directly in-front of the detector, however for most other cases we rely on diffuse reflection to scatter light back to the detector when the angle of incidence is not orthogonal to the surface.

When light meets a surface there are three options that can occur, it can be absorbed as energy, transmitted as light into the new medium, or reflected back into the medium it came from.

Generally, darker objects absorb more light, and lighter ones reflect more. This is not a rule for the IR spectrum, as other factors come into play, however in practice it is still observed to have a noticeable effect.

2.3 LiDAR

(This section serves as a summary of some basic background theory, for more details see: [9],[10],[3].)

Light Detection and Ranging (LiDAR), using the principle of time of flight to make detections of objects. There are three main categories of LiDAR; Direct Time-of-Flight, Range-gated Imaging, and Phase Difference Measurement. [9]

2.3.1 Direct Time-of-Flight

In the direct time-of-flight measurement method, a discrete pulse is emitted starting a timer, which is then stopped by the returning echo. Since the speed of light does not vary significantly under operating conditions, this time difference can be directly converted to a distance using Equation 2.1, where C is the speed of light ($\approx 3 \times 10^8$).

$$d = \frac{C \times t}{2} \tag{2.1}$$

The time intervals that have to be measured to achieve accuracies on the order of a centimetre are only 67 ps in length, and therefore ordinarily rely on analogue measurements.[9]

(fig 2) shows the outgoing signal and incoming echo, with three points of note. The

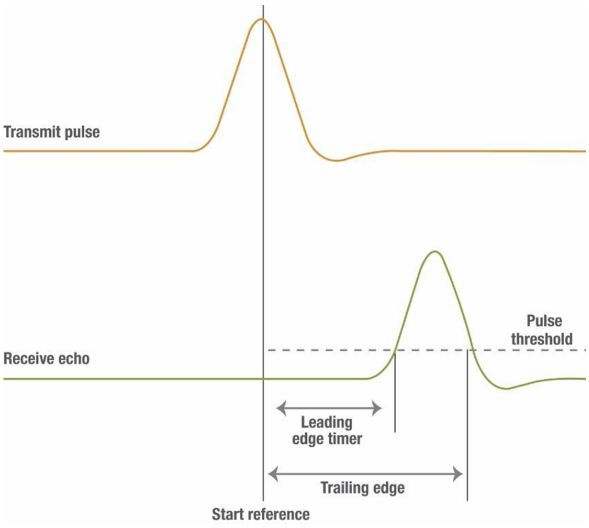

Figure 2: Diagram of Signal and echo taken from LedderTech White paper [9]

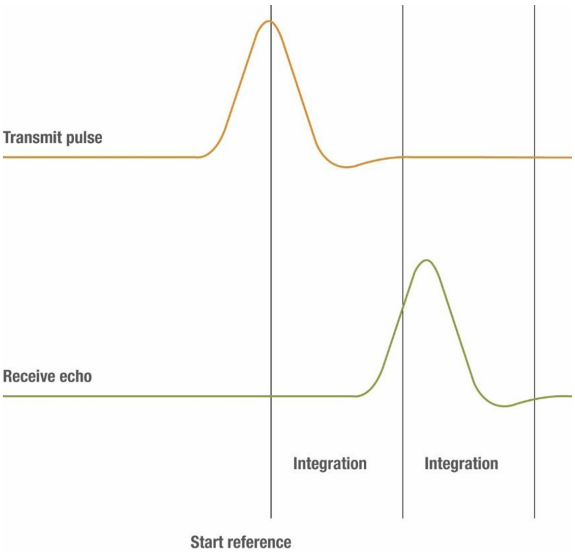

Figure 3: Diagram of range-gating taken from LedderTech White paper [9] LeddarTech

peak of the signal is the start reference point, that would start the timer. To locate an object a threshold is used, and the leading and trailing edges show when an object echo crosses the threshold.

2.3.2 Range-gated Imaging

Range gating is a simple solution to the problem identified in Direct-ToF. Instead of trying to measure the exact time the echo crosses the threshold, the energy received in a window of time is recorded for a series of time intervals, and then used to determine which interval the waveform is dominantly in. (fig 3)

2.3.3 Phase Difference Measurement

Phase difference relies on a modulated signal, rather than a short wave packet. The phase difference between the outgoing signal and the echo is used to determine the distance according to equation 2.2.

$$d = \frac{C \times \Phi}{4\pi \times f} \tag{2.2}$$

Where Φ is the phase difference and f is the modulation frequency.

This can provide a more accurate result, but also has the possibility of the phase difference being greater than 2π, resulting in far away objects appearing substantially closer.

2.4 LeddarTech

Unlike traditional Direct-ToF LiDAR, LeddarTech do not use analogue signals to start and stop their timer. They sample across the entire range of the detector, build-

ing an intensity profile of incoming light. Using patented methods they then iteratively expand the sample rate and resolution of the signal, before analysing the resulting time signal . By default, this signal plot would have one datapoint every $4.8m$. However, LeddarTech uses an oversampling technique, repeating the signal output and echo analysis, collecting data with the same frequency but offset from the previous measurements, allowing for a better picture to be created. (fig 4) The number of samples used for a single output can be selected by the user, with the trade-off being greater accuracy with higher oversampling, but increased latency, and potential artifacting for moving objects. Leddartech recommends against oversampling for objects moving faster than $1m/s$.

2.4.1 M16-LSR [6]

The specific model unit used for these experiments is the M16R-75J0008. It has a 16-segment horizontal detector array, with each detector having a $3° \times 3°$ field of view, resulting in an overall 48° wide field of view.

It has a stated accuracy of $\pm 5cm$, and range of $60m$ for a retroreflector, and $10m$ for a Kodak Gray Card of 18% reflectivity. This difference in range dependant on object reflectivity is important to note and will be discussed later.

2.5 Experimental theory

Before determining features with LiDAR, the setup in question must be understood. For this case the LiDAR is a 2D flash LiDAR, that emits a pulsed diverging beam, and returns the ToF for each of sixteen detectors each measuring a 3° arc. These arcs cover an unbroken 48° Field of view (FoV), however they can only return the distance of the nearest point in their view as utilised.

These arcs of radius r, can be approximated to triangles, resulting in a maximum error of $3.4 * 10^{-4} * r$ at the centre of the arc.

This approximation dramatically simplifies the processing of data for feature analysis, but also turns out to be pretty much irrelevant. Due to the fact that the detectors return the distance of the nearest point in the FoV, if an arc is incident on a flat surface at an angle other than 90°, the distance returned will correspond to one of the corners of the arc.

2.6 Feature determination [11]

Once points have been determined from the detector outputs, feature determination occurs. Feature determination follows a sequence as follows:

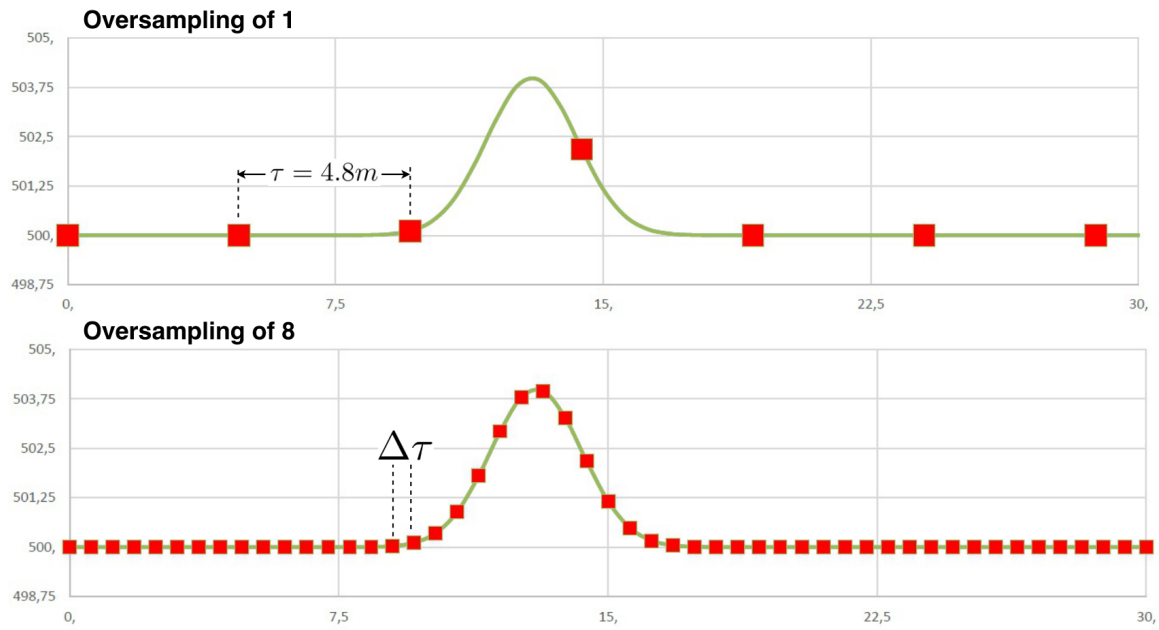

Figure 4: Diagram of oversampling method taken from Godejord, Børge [10], originally taken from LeddarTech corporate presentation that can no longer be accessed

2.6.1 Seeding

Two points in series are compared, and a line is fit to them to test if there is a straight edge feature. Using the function of this line a prediction is made as to where the next point on this line should be as seen by the LiDAR. This prediction is then compared to the actual next point, and if it is within a tolerance, the three points are grouped as a seed. This is tried for every point.

2.6.2 Seed Growth

Once there are no more seeds to be found, each seed goes through a growth algorithm similar to the original seeding one. This time a line of best fit is found for the three points in the seed, and a prediction is made for the adjacent points not in another seed, which is then compared to the actual points. This process repeats for all points, adjusting the best-fit line for each point added.

2.6.3 Seed joining

A new function compares seeds and joins them if appropriate. For example if two seeds share a point, and have a similar slope, they would be joined.

2.6.4 Corners

A function for determining corners where line features intersect. This can also cover the case where two seeds share a point, and yet their slopes are substantially different.

3 Method

The overall aims of the practical experiments were to gather data that could be used for investigating the accuracy and usefulness of the LiDAR sensors being used.

3.1 Experiment (1)

Aim: To verify how the detectors operate.

The setup for this experiment involved mounting a LiDAR unit to a photonics bench, with a photodetector in front of it configured to an Oscilloscope

- First a handheld amplitude sensor was held directly in-front of the laser output to give a rough intensity value, and confirm laser safety for use outside of the lab.
- Next, Align the vertical height of the laser output to the photodetector using an infrared laser viewing card to locate the beam.
- Then the horizontal angle of the laser was adjusted to achieve the highest output from the photodetector.
- A cable with a resistivity of 50Ω was used to connect the photodetector to the oscilloscope in line with the detectors specifications to achieve a sample rate of $3.142 \times 10^{-10} s$

3.2 Experiment (2)

Aim: to practice recording data and determine the effectiveness of a single detector in the array when detecting a small object.

The setup involved directing the LiDAR unit down a long corridor, with a retroreflector positioned towards the end.

- Centre one of the middle detectors parallel to the length of the corridor by finding the highest detected range when rotating from one wall to the other.
- Take a snapshot of the detectors view with a retroreflector being held at known distance at the end of the corridor.
- Cover the retroreflector in paper and take another snapshot, so as to have the same item in frame with lower reflectivity.

3.3 Experiment (3)

Aim: To collect data in a large room and improve on the usefulness of this data from the previous experiment.

The sensors were configured with no oversampling due to the expectation that they would be detecting moving objects which cannot utilise that funciton.

1. LiDAR sensors positioned 180cm apart

(approximately the width of the most common small cars such as VW Polo, Ford Fiesta, etc.

2. Dimensions of the room were measured, including the position of the LiDAR sensors within it and any notable features that could affect the sensors, in this case a metre tall stage.

3. A grid was marked out infront of the sensors.

4. A snapshot was taken with a person in each position on the grid.

5. These snapshots were repeated for a variety of setups, by angling the detectors inwards (reducing blind spot infront of car at expence of overlap in peripheral vision) and by reducing the separation of the detectors, to evaluate the importance of separation on accuracy.

4 Theoretical Method

In this section the coding aspects of the project will be explained. The focus will predominately be on the fourth experiment.

4.1 Data Handling

A large part of this project was just handling the large amounts of data. The aim was to make it simple and quick to access for later analysis steps.

1. Import the labview data folders

2. Using OS module, search through the data directory for all LVM type files and process the two data columns into numpy arrays. From here they were each assigned a value for theta based on their position in the detectors array, which can be updated with an offset later.

3. At this point, the reconfigured raw data is saved as a CSV for each file to speed up the later stages.

4. New data is inferred from the raw data, using the known origin of each detector, and X, Y position is assigned in addition to the polar coordinates. And theta is updated with an offset where applicable.

5. Intensity is scaled based on the recorded radial distance

6. Finally any points with an Intensity of zero are given a distance of $10,000cm$, the assumption being that there is nothing in the line of sight of the detector. Though, at many stages in the analysis these points will be excluded and not assumed to be accurate.

7. Each of the 11,520 data points were manually marked as being apart of either a wall, or object, to allow for

accuracy to be determined for each. This was done on a per detector basis, so each of the 32 detectors would be looked at individually, and if for a given object location the corresponding reading was in the vicinity of said object, and exceptionally far from its modal location in that dataset, then that reading is associated with that object.

4.2 Raw Accuracy (fig 5)

Before investigating any advanced computational methods to improve accuracy or object identification, it is important to identify the accuracy of the sensors.

1. for each detector, each sensor, a mask is created centred along its FoV, though a degree narrower (this is due to the nature of how the detectors return their distances, using a waveform which must have a non-infinitesimal length).

2. The object (a person) is approximated to be an elliptical shape of 40cm width and 15cm depth. This object is positioned with the front most surface at the objects recorded location as was setup in the experiment.

3. These binary masks are multiplied, returning a mask of only their overlaping area. The average distance between the sensors origin and the closest second through eleventh pixels is returned as the empirical distance.

4. Each sensor with the object in their FoV (and non-zero intensity) then has a difference between empirical and recorded distance returned, which can then be analysed using a histogram for each setup. The results should be consistent, as there is no dependence on triangulation at this point, and any discrepancies demonstrate a systemic flaw in the different setups.

For data-points marked as detecting a wall rather than an object, empirical distance is calculated as the distance to the wall from the detector origin at the angle of the centre of that detector's FoV.

4.3 Walls

As covered in the Theory section, there is a process of seeding, growing, and connecting line segments to identify walls in the sensors view. This is an advanced computational method to improve the usability of the limited data...

All data-points in a snapshot are converted from polar to Cartesian co-ordinates. Then they are run through a function that takes each group of three points, draws a line between the first and third point and

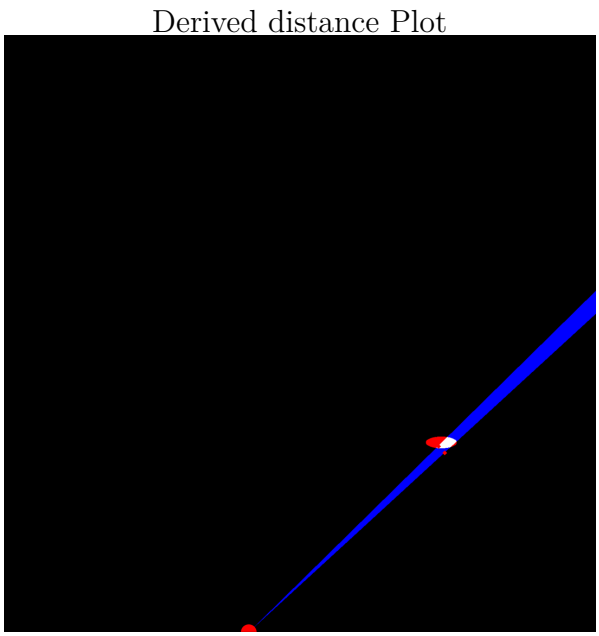

Figure 5: Plot shows detector FoV in blue, Object in red, and overlap in white

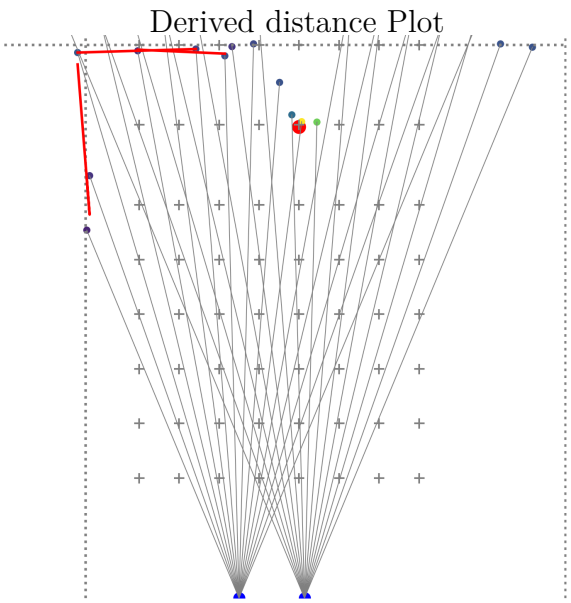

Figure 6: Plot shows walls in red

compares the perpendicular distance of the second point from the line to an acceptable error value. This value can be determined once the accuracy results have been characterised.

5 Results

5.1 Experiment (1)

At zero distance the laser output was approximately $10mw$, at $905nm$ wavelength. This confirmed its classification as a class 1 laser considering its diverging beam. The frequency of pulses from the laser were measured at $50,000Hz$, though the width of each pulse was measured on the order of $25ns$

5.2 Experiment (2)

The results of Experiment 2 show a side-by-side of a control snapshot of the corridor, a control with a covered retro-reflector, and an uncovered retroreflector. (fig 8)

The control and covered retro-reflector had a maximum recorded distance of $1276cm$, whereas the retro-reflector recorded $1142cm$

5.3 Experiment (3)

The results of Experiment 3 are far more substantial than the other experiments. There are five sets of data, each with 72 subsets of 32 points. A plot of the raw position data for on subset of points, with the object location marked, can be seen in (fig 9)

Not all detectors returned a value, instead returning zero intensity and distance. This

Osciliscope Screenshots experiment (1)

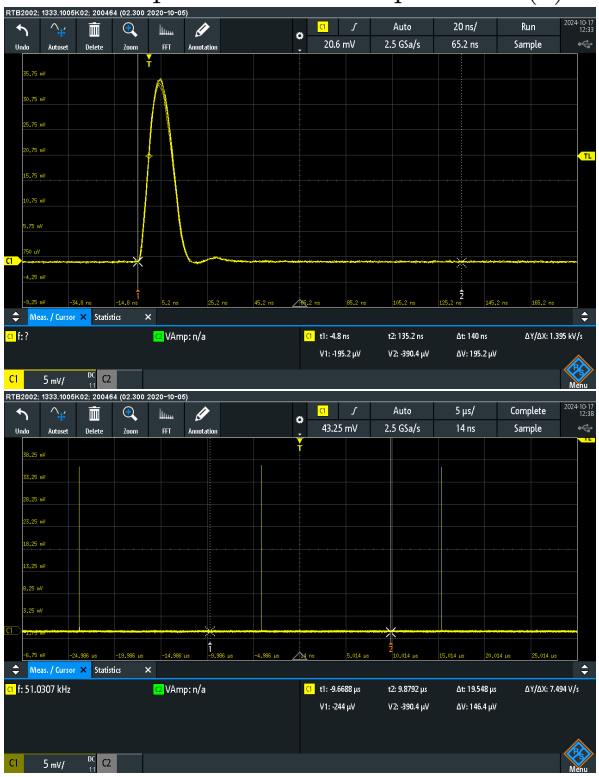

Figure 7: Osciliscope output where higher shows the width of a single pulse and lower shows time between pulses.

varied with each recording and did not represent a broken apparatus or systemic problem.

6 Discussion of Results

6.1 Experiment (1)

The results from experiment 1 show the laser to be quite powerful, outside of the safety limits for a narrow beam. However due to the divergence of the beam this power drops off drastically with distance.

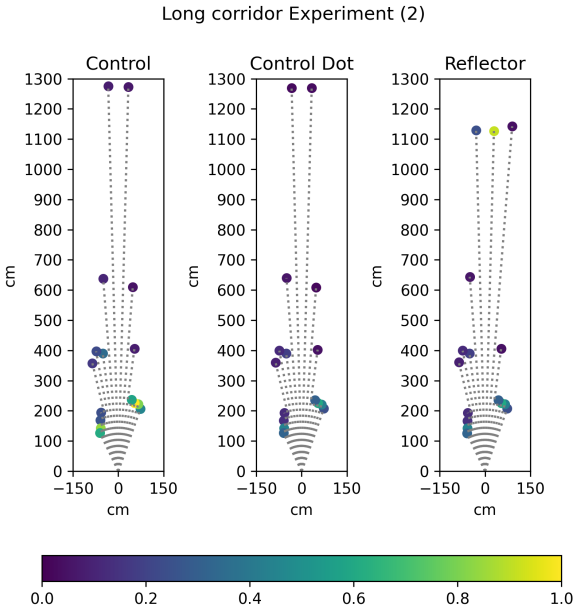

Figure 8: Long Corridor data with three comparisons.

6.2 Experiment (2)

The results from experiment 2 (fig 8) showed something unusual. In the first and second control readings, the distances measured were near identical, with the maximum recorded distance of both being $1276cm$. However, in the third reading the maximum distance was $1142cm$. This is in spite of the fact that the second and third readings are viewing an object in the same location, in-front of the wall that from the control reading.

I believe this can be explained by the intensity reading. The retroreflector is a very small object, though returns a high intensity echo signal. When this is analysed within LeddarTech's processing unit, it will be an obvious enough peak to return an object.

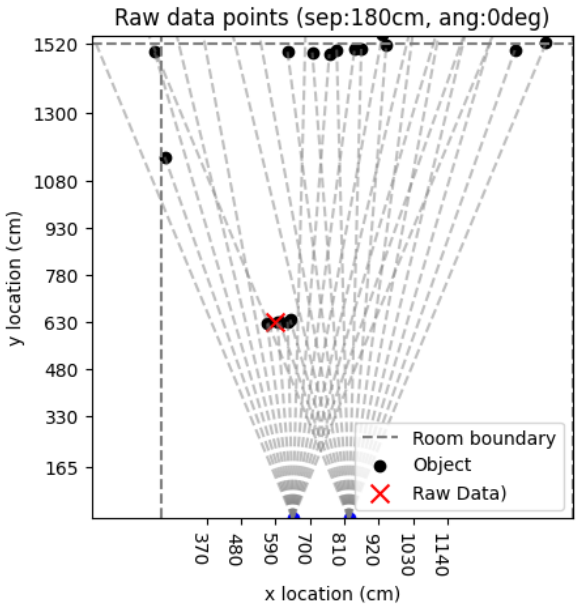

Figure 9: Raw data for Exp 3

When that intensity is taken away, however it will be a small fluctuation in the intensity profile of the echo signal. The equally low reflectivity wall will have a much greater intensity due to the amount of area in the detector's FoV it will return light from.

This raises a concern when considering relatively small pedestrians when in-front of much larger, more reflective objects.

6.3 Experiment (3)

As discussed in the Theoretical method section, the raw data from experiment 3 were categorised into walls and object readings for the purpose of determining sensor accuracy, and visualising any systemic errors such as in the sensor angle or location.

For wall readings, the errors were higher than expected, and largely dependant on the sensor angle, suggesting a systemic error in the setup process. (fig 10)

Once the angles of the individual sensors were adjusted, it was possible to reduce the standard deviation to closer to that of the zero angle offset results, which were $31.63cm$.

The calculation of the means and standard deviations for wall readings were done as outlined in the Theoretical Method section. And the SciPy.stats.Norm module was used to fit a Gaussian distribution to the errors.

Walls 180cm Separation, 0° offset

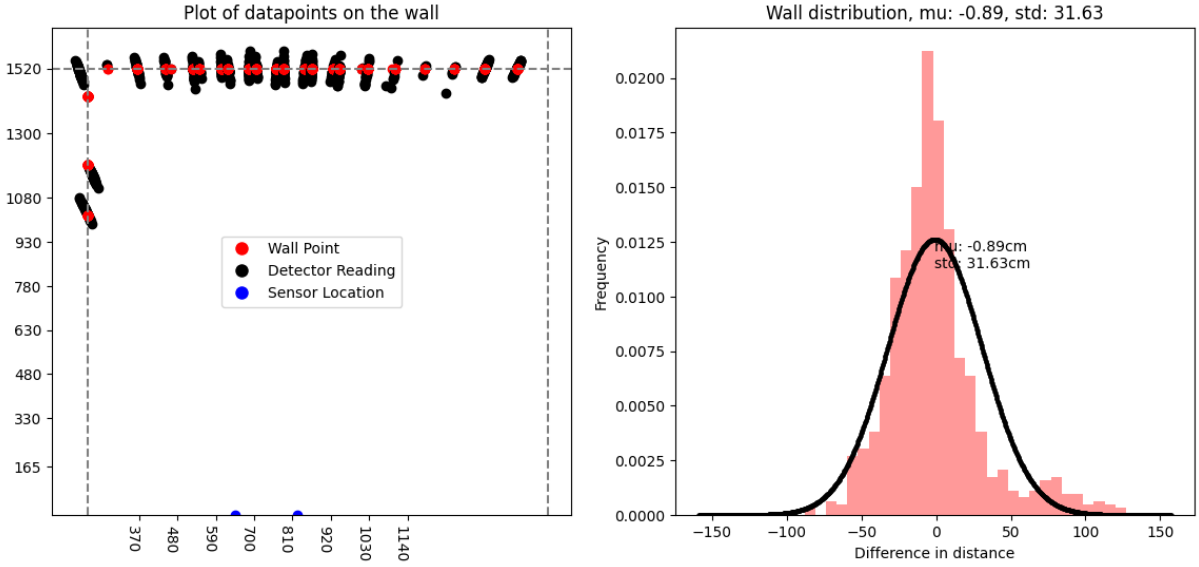

Walls 180cm Separation, 29° offset

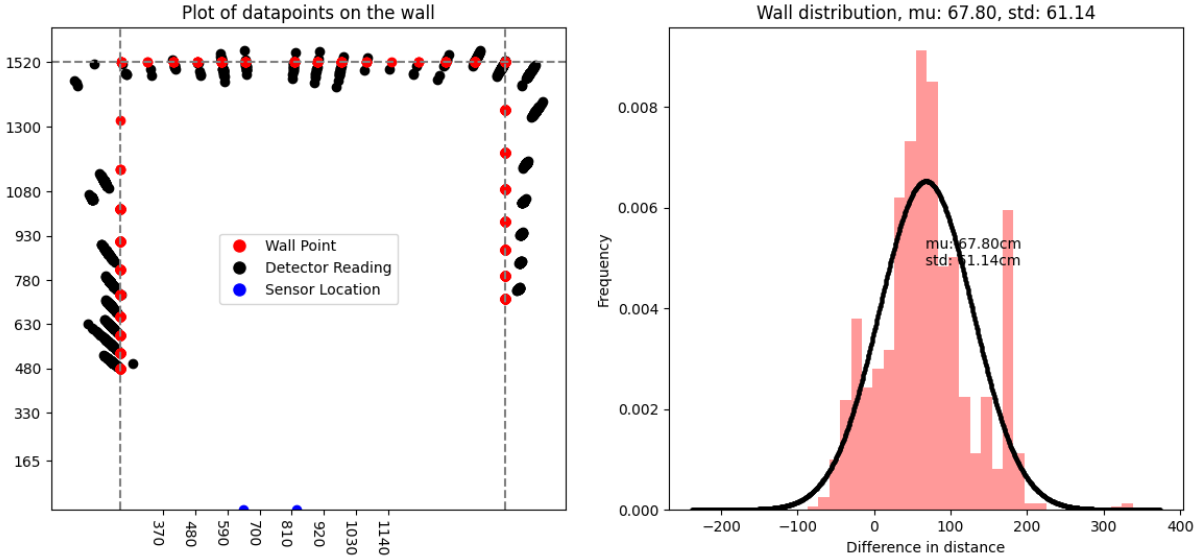

Walls 90cm Separation, 24° offset

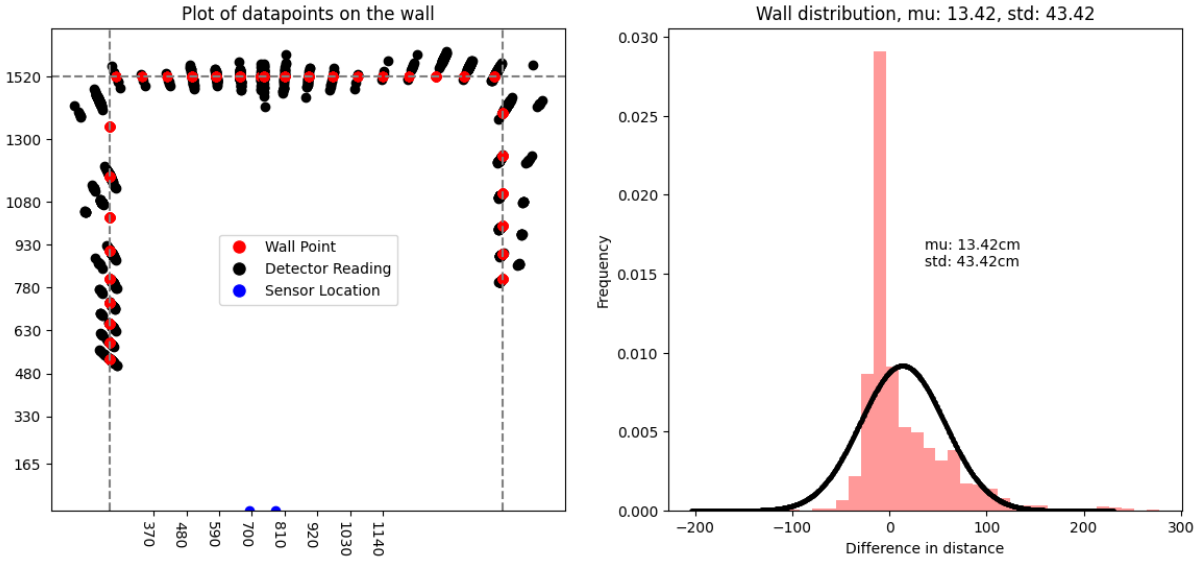

Figure 10: Experiment (3), Walls results

The points data was analysed in much the same way, with the empirical distances calculated as outlined in the Theoretical Method. However, due to difficulties in separating the readings taken when the object was up against the wall, these readings were not factored into the Gaussian fit, but are still included in the histogram for completeness. (fig 11)

The outcomes of these results were far superior to the wall readings. With consistent standard deviations between $8.19cm$ and $9.55cm$, and a mean value exceptionally close to zero.

There are two contributing factors to this discrepancy.

1. The method of determining empirical distance, though equally effective in absence of systemic errors, will have a different effect in the presence of such errors.

   For the object readings, if the object is in the detectors FoV, it will return the distance to the object. If the angle offset is systemically inaccurate, it will still return the same empirical distance so long as that angular error is corrected to within the FoV of the detector.

   For wall readings, if the angle offset is wrong, the empirical distance will be taken from a different point on the wall. This point will have a different distance to the point that was really being measured. And this effect is substantially worse for the side walls due to their relative angle, which is what is seen in (fig 10)

   Even with the angle offset correctly accounted for, the returned reading will not necessarily be from the centre of the detector's FoV, producing the same effect to a reduced magnitude. This again will not affect the object readings in the same way.

2. The second effect comes about as a result of the relative reflectivity of the walls and object. The object readings return a far higher intensity on average, around double that of the wall readings.

Objects 180cm Separation, 0° offset

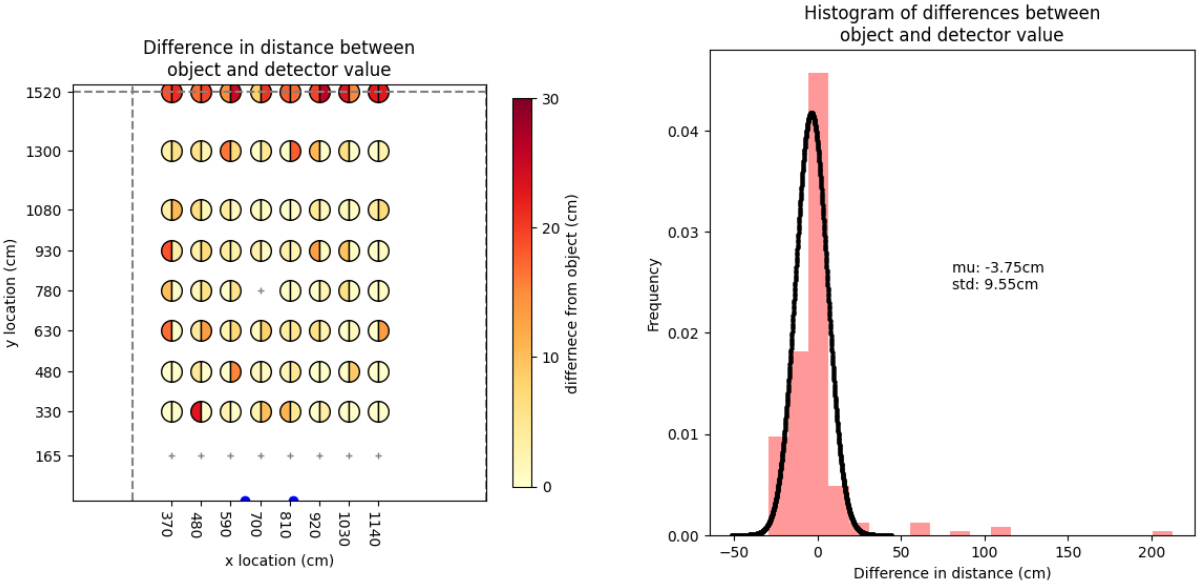

Objects 180cm Separation, 24° offset

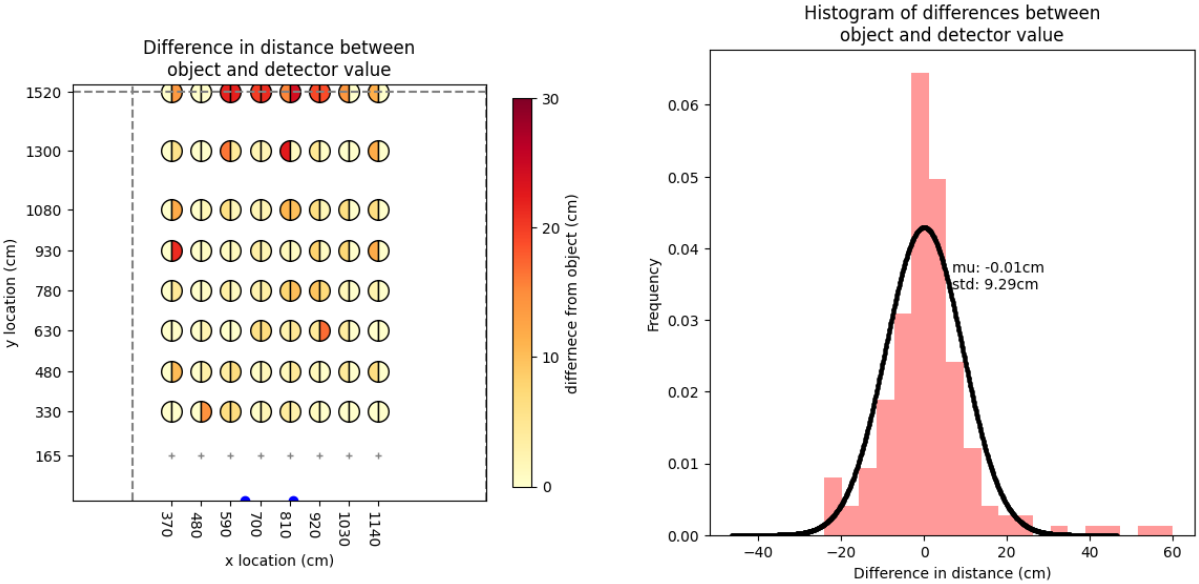

Objects 180cm Separation, 29° offset

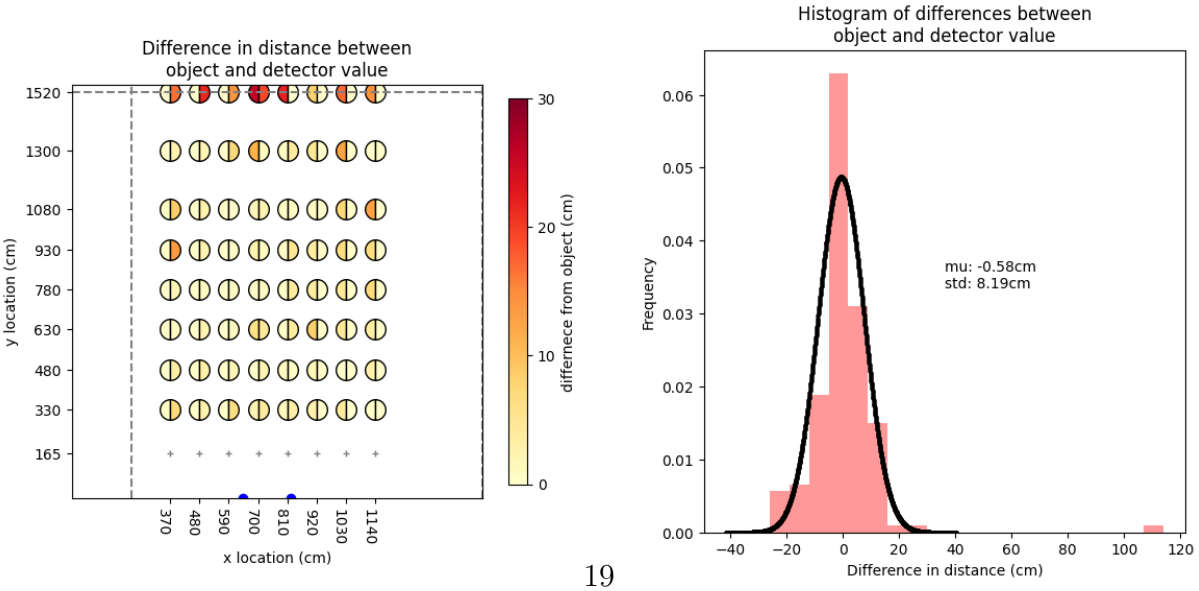

Figure 11: Experiment (3), Points results

7 Conclusion

The aim of this Thesis has been to explore the potential for LiDAR to improve road safety for all, by categorising its accuracy.

Notable from the results has been the significant dependence of accuracy on intensity. In experiment 2 it was shown that the same object in view of the detector and in front of a large white wall was seen when highly reflective, and was entirely unnoticed when covered. Returning the same result as when there was no object at all. In experiment 3 it was shown that the high intensity object returned far more accurate readings than the low intensity black walls of the environment, in spite of their large surface area.

An accuracy of $8cm$-$10cm$, though higher than the stated accuracy from the manufacturer under ideal conditions, is perfectly reasonable when determining if a pedestrian is in front of a vehicle or not. It is important too to note that in none of the object readings was the object entirely unseen except for when it was outside of the FoV of the sensors. This is a promising result for the potential use case of cheap LiDAR units.

An accuracy of $30cm$-$50cm$ is also not unusable for detecting walls of low reflectivity. Bearing in mind that a dark environment does not affect the reflectivity of the object being viewed, and so it would not be expected that night time driving would be further negatively affected.

However, the invisibility of the low reflectivity object in front of a white wall in experiment 2 does raise a substantial safety concern, if an object can go entirely unnoticed on a bright background there is potential for serious accidents. If a pedestrian stepped into the road between a large white truck and an oncoming vehicle relying on such a LiDAR system, it would need to be reliably able to detect the pedestrian.

As part of the project attempts were made to detect features using the sensors. While this worked for small sections of walls, it was inconsistent due to the limited amount of data-points provided by such a setup. To effectively locate a vehicle within a known 3D map of the environment would require a setup with far greater resolution.

Throughout these experiments, the range that has been tested has all been under $15m$. Using the two second rule of thumb for following distance this would give a maximum safe speed of $\approx 17mph$. However, not accounting for thinking time factored in for a human driver it could feasible be stretched to $30mph$, as one second is dedicated to thinking and reaction time.

This positions LiDAR as a feasible safety tool for cars in city driving when considering pedestrians, and on motorways when con-

sidering other moving, but slowing cars, removing human reaction time from the equation.

And while the consideration when collecting data was of a car mounted apparatus, the results support the potential use case of these sensors being fixed at dangerous junctions, to detect pedestrians in the road and potentially change traffic lights if needed.

References

[1] I. Baldwin and P. Newman, "Laser-only road-vehicle localization with dual 2D push-broom LIDARS and 3D priors", en, in 2012 IEEE/RSJ International Conference on Intelligent Robots and Systems (Oct. 2012), pp. 2490–2497.

[2] G. B. Times, *How much does a waymo car cost to build?*, en-US, Apr. 2024.

[3] Y. Li and J. Ibanez-Guzman, "Lidar for Autonomous Driving: The Principles, Challenges, and Trends for Automotive Lidar and Perception Systems", IEEE Signal Processing Magazine **37**, Conference Name: IEEE Signal Processing Magazine, 50–61 (2020).

[4] S. Royo and M. Ballesta-Garcia, "An Overview of Lidar Imaging Systems for Autonomous Vehicles", en, Applied Sciences **9**, Number: 19 Publisher: Multidisciplinary Digital Publishing Institute, 4093 (2019).

[5] *Infrared radiation | Definition, Wavelengths, & Facts | Britannica*, en, Dec. 2024.

[6] *LEDDAR M16 Datasheet*, English, May 2017.

[7] *The Role of Infrared Sensors in Light Detection and Ranging - LiDAR*, en.

[8] J. Lekner, *Theory of reflection: of electromagnetic and particle waves*, eng, Open Library ID: OL2730450M (M. Nijhoff Publishers, Dordrecht, Boston, Hingham, MA, USA, 1987).

[9] *Leddar-Optical-Time-of-Flight-Sensing-Technology*, English, 2016.

[10] B. Godejord, "Characterization of a commercial LIDAR module for use in camera triggering system", eng, MA thesis (2018).

[11] H. Gao, X. Zhang, Y. Fang, and J. Yuan, "A line segment extraction algorithm using laser data based on seeded region growing", en, International Journal of Advanced Robotic Systems **15**, Publisher: SAGE Publications, 1729881418755245 (2018).